



ELSEVIER

Thermochimica Acta 257 (1995) 149–161

thermochimica
acta

Thermal analysis of some complexes with malonamide

S.H.J. De Beukeleer^a, H.O. Desseyn^{a,*}, S.P. Perlepes^b, J. Mullens^c

^a Department of Chemistry, Universitair Centrum Antwerpen, Groenenborgerlaan 171,
B-2020 Antwerp, Belgium

^b Department of Chemistry, University of Patras, 26010 Patra, Greece

^c Limburgs Universitair Centrum, Department SBG, Universitaire Campus, B-3590 Diepenbeek, Belgium

Received 3 May 1994; accepted 8 November 1994

Abstract

In alkaline medium, malonamide forms anionic planar complexes $[\text{ML}_2]^{2-} \cdot x\text{H}_2\text{O}$ where M is Ni or Cu. Thermograms and vibrational spectra clearly indicate that three different nickel anion complexes could be isolated, with x being respectively 2, 1 and 0. Only the monohydrate has been observed for the copper anionic compound.

Malonamide also forms neutral *trans*-octahedral $\text{M}(\text{LH}_2)_2\text{X}_2$ complexes (where M is Mn, Fe, Co, Ni, Cu, Zn; X is Cl, Br, I; LH_2 is $\text{CH}_2(\text{CONH}_2)_2$) and polymeric $[\text{Cu}(\text{LH}_2)\text{X}_2]_n$ compounds (X is Cl or Br). The neutral 1/2 complexes all decompose, forming free ligand and MX_2 by an endothermic reaction, except for Fe(II) where an exothermic reaction occurs at relatively low temperatures. The thermal breakdown of $\text{Cu}(\text{LH}_2)_2\text{Cl}_2$ and $[\text{Cu}(\text{LH}_2)\text{Cl}_2]_n$ results in new polymeric structures, exhibiting bridging chlorines. The structures proposed for these compounds are supported by infrared spectra. The thermal stability of the $\text{M}(\text{LH}_2)_2\text{X}_2$ complexes can be related to the metal–ligand bond strength and obeys the crystal field stabilization theory.

Keywords: Malonamide; TGA; Vibrational spectroscopy

1. Introduction

It is becoming increasingly apparent that the coordination chemistry of amide-containing ligands is very important for a wide variety of chemical, biological and applied systems [1]. For several years our laboratory has been engaged in the design of suitable oxamides and their complexes. In contrast to the relatively large number of

* Corresponding author.

studies in this field, practically no work, except some incomplete articles by Russian groups [2], has been published concerning malonamide. Recently we reported on the synthesis and characterization by vibrational spectroscopy of some transition metal complexes with deprotonated and neutral malonamide [1, 3]. The work presented here contains the thermal study of some deprotonated and neutral malonamide complexes using TG, DTG and DTA techniques, mainly assisted by infrared spectroscopy.

2. Experimental

We have already published the preparation of the compounds under investigation [1]. The infrared spectra were recorded on a Bruker IFS 113V Fourier Transform spectrometer. A Seiko model 200 TG/DTA was used for the thermal measurements, which were carried out under a dry nitrogen atmosphere. Simultaneous TGA–MS was used for the identification of the compounds evolved during heating. A TGA Thermobalance model 2000 951 (TA Instruments, formerly Du Pont) was coupled to a Thermolab quadrupole mass spectrometer (VG Fisons Instruments) with a mass range of 1–300 amu. This mass spectrometer, which is specifically designed for thermal analysis studies, was connected to the TGA unit using a flexible, heated, silica-lined steel capillary. As TGA proceeds at atmospheric pressure whereas MS must operate below 10–5 mbar, further pressure reduction was obtained by using a molecular leak (silicon carbide frit).

3. Results and discussion

3.1. Anionic complexes $[ML_2]^{2-} \cdot xH_2O$

The anionic complexes all appear as square planar structures with D_{2h} symmetry.

Three differently hydrated nickel complexes could be isolated from the strong alkaline solutions, namely $K_2[NiL_2] \cdot 2H_2O$ (A), $K_2[NiL_2] \cdot H_2O$ (B) and the water-free compound $Na_2[NiL_2]$ (C). The TG curves for product A at different heating rates are given in Fig. 1. After a loss of weight equivalent to two water molecules in well-defined steps, the water-free compound, hereafter called product D, remains stable up to approx. 250°C and starts to decompose at higher temperatures without formation of any stable intermediate.

The activation energy, calculated according to Flynn and Wall [4] and Wendlandt [5], is shown in Table 1. As could be expected, the activation energy for the release of the second water molecule is much higher than for release of the first. Comparing the temperatures and activation energies for dehydration processes from similar complexes does not lead us to any clear conclusion about the bonding characteristics of the water molecules. Nevertheless, the spectra, especially the splitting of the (NH) fundamentals, indicate that the water is hydrogen-bonded to the ligand.

Product B releases one mole of water over a wide temperature range (Fig. 2), clearly indicating different types of water in this compound. No stable product is formed after

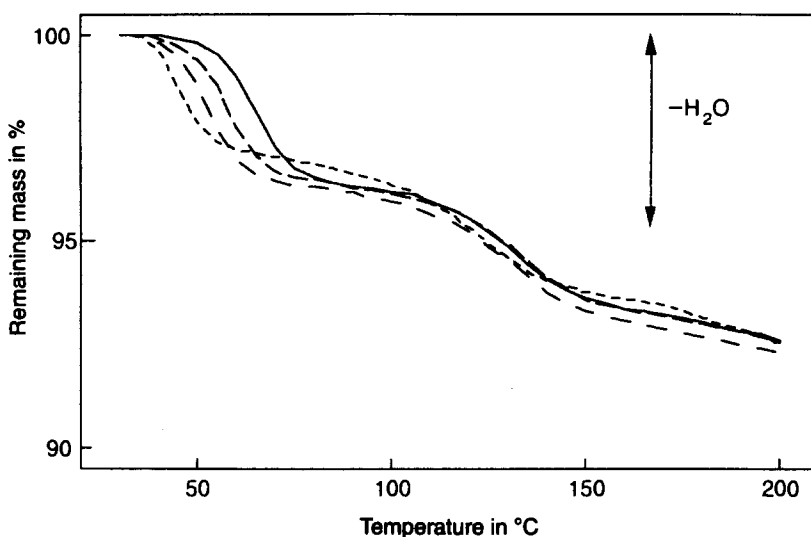


Fig. 1. TG curves for $K_2[NiL_2] \cdot 2H_2O$ (A) at different heating rates: ---, $1^\circ C \text{ min}^{-1}$; ———, $5^\circ C \text{ min}^{-1}$; - - - - , $10^\circ C \text{ min}^{-1}$; ———, $20^\circ C \text{ min}^{-1}$.

Table 1

Calculated activation energy (kJ mol^{-1}) for the two steps of dehydration of $K_2[NiL_2] \cdot 2H_2O$ (A)

α	$(E_a)_1$	$(E_a)_2$
0.1	158	179
0.2	151	178
0.3	144	219
0.4	139	236
0.5	137	240
0.6	136	265
0.7	136	259
0.8	148	222
0.9	158	153

dehydration. $Na_2[NiL_2]$ (C) shows no loss of water and starts to decompose above $260^\circ C$.

From these thermograms, we expect that A, B and C have different structures. This indeed is confirmed by the infrared spectra and is especially clear in the characteristic and very sensitive $\nu(NH)$ region, as can be seen in Fig. 3. $K_2[NiL_2] \cdot 2H_2O$ (A) exhibits one intense $\nu(NH)$ band at 3302 cm^{-1} , with asymmetric shoulders on the high and low frequency sides, due to the $\nu(OH)$ modes of the structured water molecules. The $\nu(NH)$ region of $K_2[NiL_2] \cdot H_2O$ (B) shows a splitting of the $\nu(NH)$ modes, indicating different types of hydrogen bonding, as could be expected from the thermogram where different

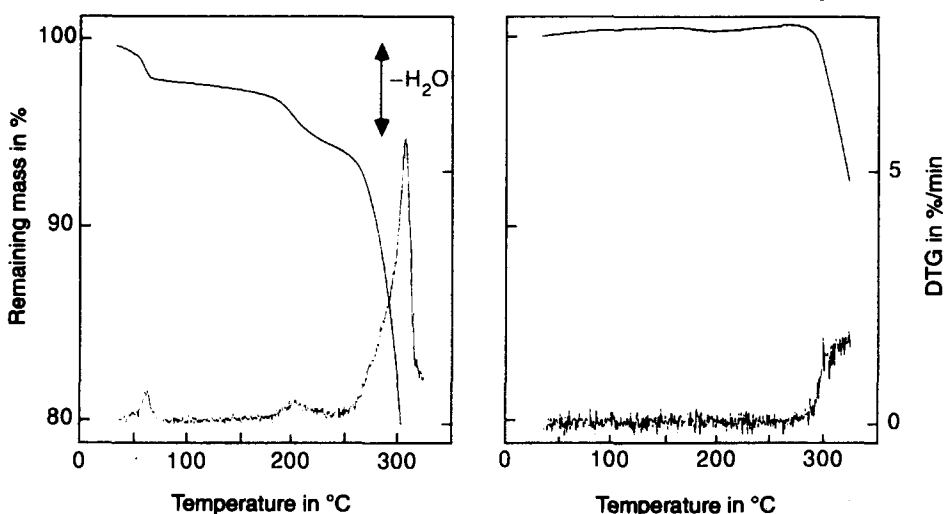


Fig. 2. TG/DTG curves for $K_2[NiL_2] \cdot H_2O$ (B) (left) and $Na_2[NiL_2]$ (C) (right).

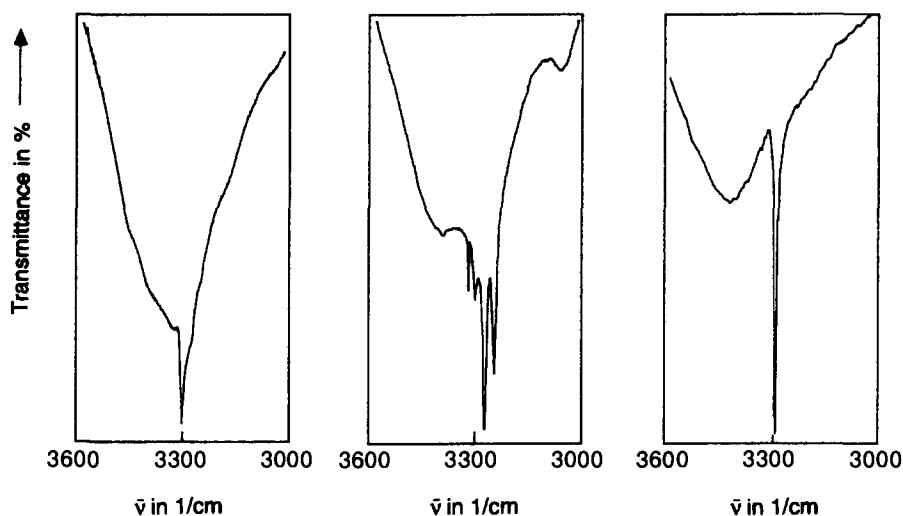


Fig. 3. The splitting of the $\nu(NH)$ bands due to hydrogen bonding to water molecules in $K_2[NiL_2] \cdot 2H_2O$ (A) (left), $K_2[NiL_2] \cdot H_2O$ (B) (middle) and $Na_2[NiL_2]$ (C) (right).

kinds of water molecules are observed. The water-free compound $Na_2[NiL_2]$ (C) exhibits only one intense $\nu(NH)$ band. This compound, however, is very hygroscopic, as can be seen from the slight increase of weight in the thermogram, even under dry nitrogen atmosphere. From the broad profile of the water band at approx. 3350 cm^{-1} , we can deduce that the water is not structured.

The fact that the water molecules in compounds **A** and **B** are indeed structured, is confirmed by the typical $\delta(\text{OH})$ and $\pi(\text{OH})$ modes at respectively 1691 and 690 cm^{-1} for **A**, and broader bands with maximum intensity at 1604 and 630 cm^{-1} for compound **B**. The broader profile of these bands in the latter confirms the theory of water molecules with slightly different surroundings. It should be noted that compound **C** and the water-free compound **D**, obtained by thermal dehydration of **A**, exhibit slightly different infrared spectra, especially in the far-infrared region, typical for lattice vibrations of slightly different crystal structures [3].

The thermograms at different rates for $\text{K}_2[\text{CuL}_2]\cdot\text{H}_2\text{O}$ are given in Fig. 4. From this figure we can state that this compound can be compared with the nickel compound **B**, as at heating rate of 1°C min^{-1} we observe different water molecules in the crystal. The infrared spectrum of the $3600\text{--}3000\text{ cm}^{-1}$ region for this copper complex (Fig. 5) also exhibits the splitting of the $\nu(\text{NH})$ fundamentals as observed for $\text{K}_2[\text{NiL}_2]\cdot\text{H}_2\text{O}$ (**B**).

The activation energy is given in Table 2. At low heating rates we can see that the dehydration of the copper complex is not a single, well-defined step but that there are, in analogy with $\text{K}_2[\text{NiL}_2]\cdot\text{H}_2\text{O}$, different kinds of water molecules present. This is the reason why the calculation of the activation energy was meaningless, i.e. there is more than one process involved. However a comparison of the temperatures at which dehydration takes place might lead us to some conclusions. As can be observed in Fig. 4, the copper complex has lost all its water at approx. 130°C while the dehydration of $\text{K}_2[\text{NiL}_2]\cdot\text{H}_2\text{O}$ does not reach completion until approx. 230°C (Fig. 2(a)). This means that the water molecule in $\text{K}_2[\text{CuL}_2]\cdot\text{H}_2\text{O}$ is less firmly bound to the complex, which had been indicated by the positions of the $\nu(\text{NH})$ and $\nu(\text{CO})$ fundamentals in the IR spectra of these compounds [3]. Indeed, we can observe $\nu(\text{NH})$ and $\nu(\text{CO})$ at higher

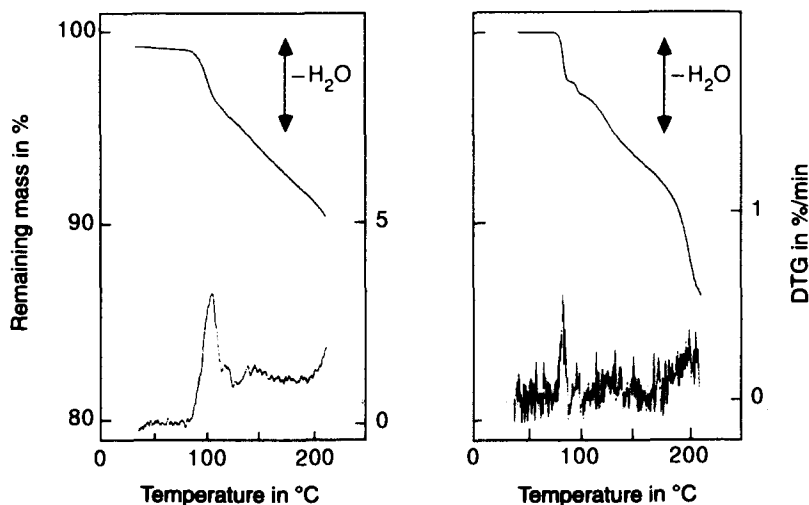


Fig. 4. TG/DTG curves for $\text{K}_2[\text{CuL}_2]\cdot\text{H}_2\text{O}$ at different heating rates: $20^\circ\text{C min}^{-1}$ (left) and 1°C min^{-1} (right).

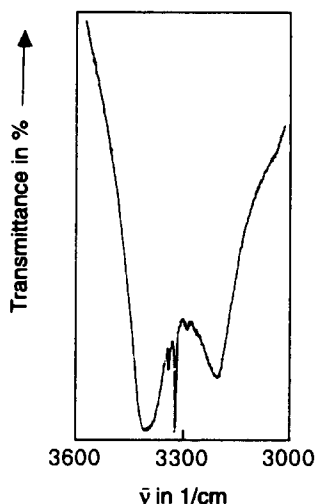
Fig. 5. $\nu(\text{NH})$ region for $\text{K}_2[\text{CuL}_2]\cdot\text{H}_2\text{O}$.

Table 2

Calculated activation energy for the dehydration of $\text{K}_2[\text{CuL}_2]\cdot\text{H}_2\text{O}$

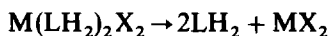
α	$E_a/\text{kJ mol}^{-1}$
0.1	262
0.2	201
0.3	183
0.4	172
0.5	169
0.6	221
0.7	261
0.8	294
0.9	251

wavenumbers for $\text{K}_2[\text{CuL}_2]\cdot\text{H}_2\text{O}$, proving weaker intermolecular interactions, i.e. hydrogen bonding, between the amide function and the water molecule.

3.2. Neutral complexes $\text{M}(\text{LH}_2)_2\text{X}_2$

The thermograms for $\text{Mn}(\text{LH}_2)_2\text{X}_2$ are given in Fig. 6; the $(\Delta m/\Delta t)_{\text{max}}$ for the chloride is observed at 250°C, for the bromide at 264°C, and for the iodide compound at 269°C. This sequence for halogen substitution is also observed for the other metals.

The Co, Ni and Zn complexes all decompose in a similar way as $\text{Mn}(\text{LH}_2)_2\text{Cl}_2$, by the loss of weight of two ligands in an endothermic reaction



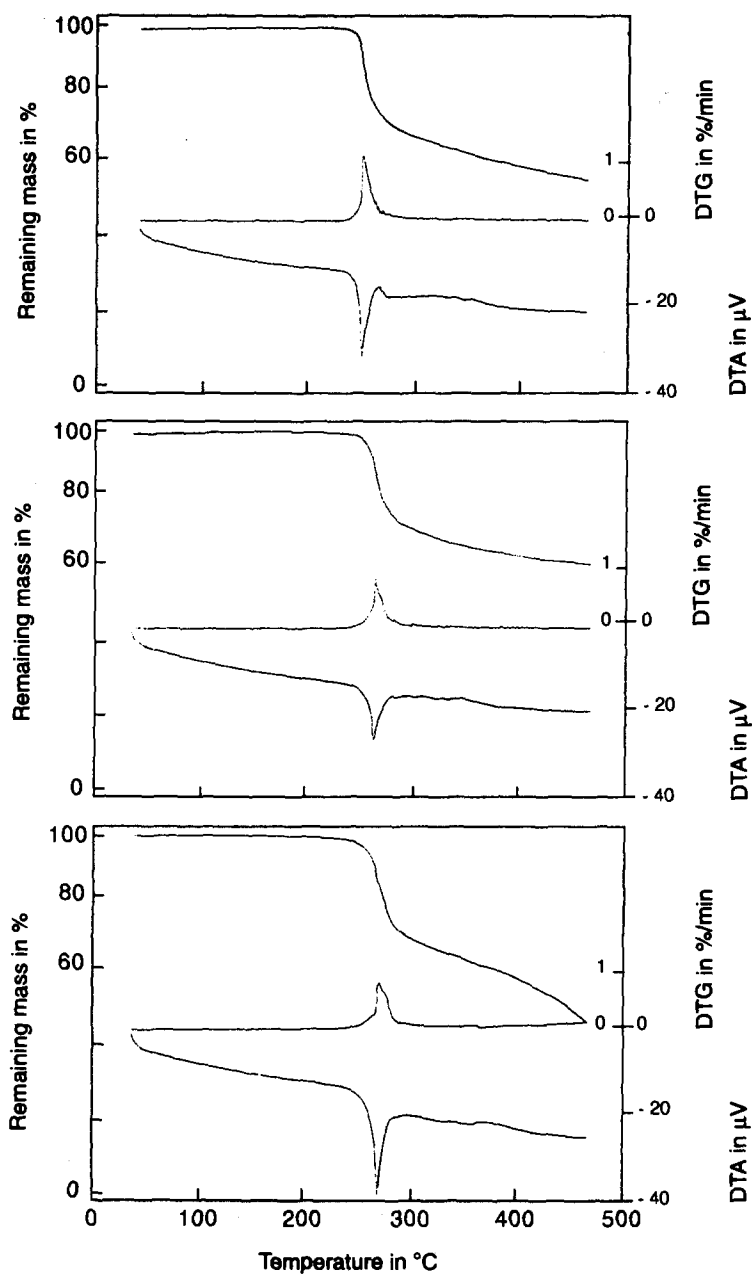


Fig. 6. TG, DTG and DTA curves for $\text{Mn}(\text{LH}_2)_2\text{X}_2$: upper, X is Cl; middle, X is Br; and lower, X is I.

During this process, because the infrared spectra of the products after a loss of weight of respectively 15%, 20% and 30% are identical, no intermediates are formed.

The thermal decomposition of $\text{Fe}(\text{LH}_2)_2\text{Cl}_2$ is given in Fig. 7. Infrared [3] and Mössbauer spectra [1, 6, 7] also indicate a monomeric distorted octahedral structure for this compound. Its thermal degradation, however, is completely different from the others: the first step consists of an exothermic process followed by an endothermic one, which is probably due to the oxidation of Fe(II) to Fe(III). No stable intermediates were formed during the decomposition.

The copper complexes do form new stable compounds; they are discussed below.

Table 3 lists the $\nu(\text{metal-ligand})$ and $\nu(\text{metal-chlorine})$ fundamentals for the different complexes and shows the effect of the weak crystal field stabilization energy on the frequencies in this series [3]. The high $\nu(\text{Cu-ligand})$ and low $\nu(\text{Cu-Cl})$ fundamentals are very well explained by the tetrahedral distortion caused by the Jahn–Teller effect [8]. This effect results in a different thermal behaviour of the copper complexes. The $(\Delta m/\Delta t)_{\text{max}}$ values also correspond very well to the weak field stabilization energy

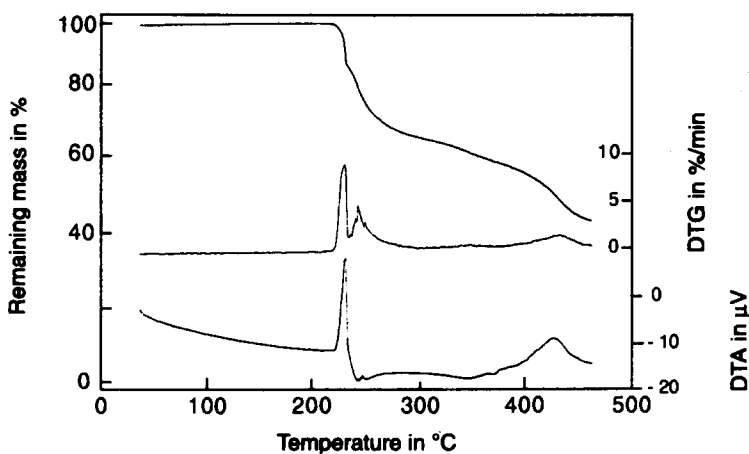


Fig. 7. TG, DTG and DTA curves for $\text{Fe}(\text{LH}_2)_2\text{Cl}_2$.

Table 3

Crystal field stabilization energy, affirmed by far-infrared spectra and differential thermogravimetry

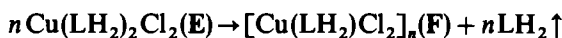
	$\nu(\text{M-O})/\text{cm}^{-1}$	$\nu(\text{M-X})/\text{cm}^{-1}$	$(\Delta m/\Delta T)_{\text{max}}/^\circ\text{C}$
Mn	257	158	250
Fe	264	165	
Co	275	172	258
Ni	290	183	318
Cu	[310]	[178]	
Zn	287	181	244

sequence. An increase in this energy results in a more stable compound, which is in turn reflected in higher $\nu(\text{metal-ligand})$ modes. As the decomposition of these complexes occurs at the metal–ligand bonding, by releasing the malonamide from the metal, we consequently expect a higher temperature for the degradation of the more tightly bound species.

3.3. Copper complexes

The thermogram of the monomeric pseudo-octahedral $\text{Cu}(\text{LH}_2)_2\text{Cl}_2$ (**E**) is given in Fig. 8. The first step is an endothermic process, followed by an exothermic one; the intermediate further decomposes to form CuO . The isothermal process at 176°C , given in Fig. 9, clearly shows the formation of a stable intermediate (**F**), after a loss in weight of approx. 30%, corresponding to one mole of ligand. During this process, a white condensate was formed on the exit of the oven tube, identified by infrared spectroscopy as free malonamide. Infrared spectra of the intermediate show, besides the fundamentals of coordinated malonamide, a few new bands at approx. 140 cm^{-1} , typical for bridged metal–chlorine modes, indicating a polymeric structure for this compound. The terminal $\nu(\text{Cu-Cl})$ modes at approx. 180 cm^{-1} observed for the monomeric $\text{Cu}(\text{LH}_2)_2\text{Cl}_2$ have disappeared (Fig. 10).

According to these results the formation of the intermediate can be given by the equation



The temperature of formation of the intermediate is very critical as lower temperatures give practically no decomposition of the starting material and direct decomposition of the intermediate occurs above 176°C (Fig. 9).

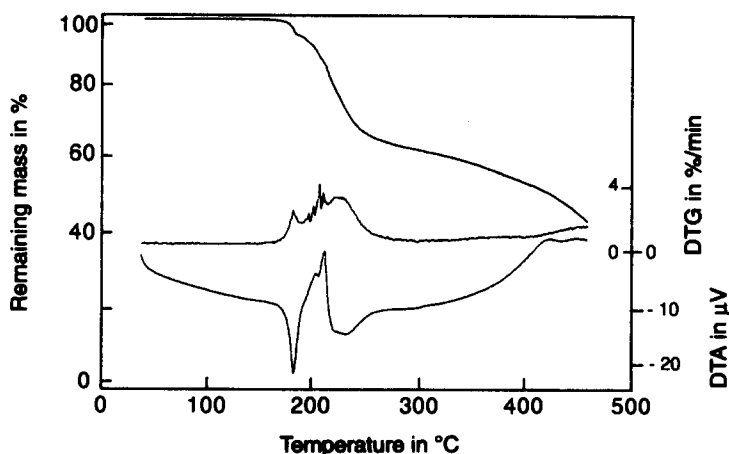


Fig. 8. TG, DTG and DTA curves for $\text{Cu}(\text{LH}_2)_2\text{Cl}_2$ (**E**).

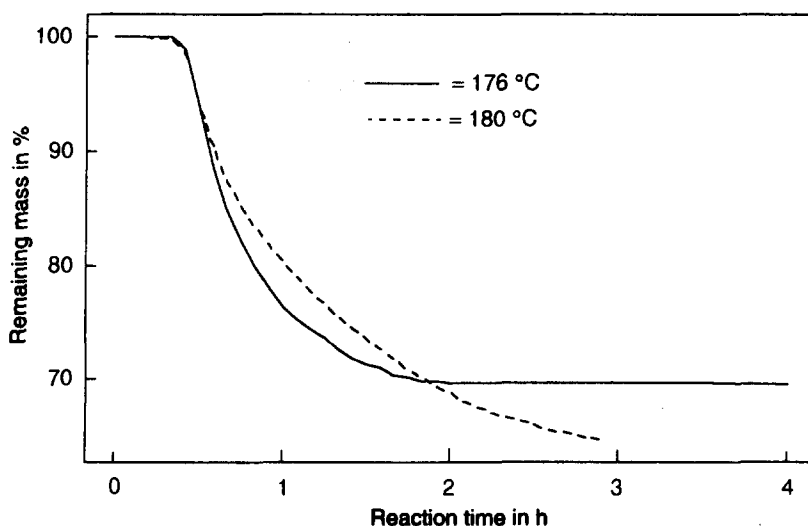


Fig. 9. Isothermal measurements on $\text{Cu}(\text{LH}_2)_2\text{Cl}_2(\text{E})$ at 176°C and 180°C .

Such an intermediate cannot be formed from $\text{Cu}(\text{LH}_2)_2\text{Br}_2$ as the decomposition of this 1/2 compound starts at higher temperatures compared with the chlorine analogue and the polymer intermediate is no longer stable at this elevated temperature. Isothermal processes at different temperatures, to prepare the bridged bromine compound, were unsuccessful.

The thermogram of $\text{Cu}(\text{LH}_2)\text{Cl}_2(\text{G})$, prepared in the laboratory, is given in Fig. 11. Isothermal analysis, given in Fig. 12, suggests a new stable intermediate (H), after a loss of weight equivalent to 2/5 of the ligand. During this degradation, no malonamide, but traces of NH_3 , CO_2 and H_2O , were observed in the mass spectrum of the evolved gasses, indicating a decomposition of malonamide. As no chlorine traces were detected, we can be sure that the loss of weight in this process is due only to the thermal breakdown of the ligand itself. These isothermal experiments are very interesting and clearly show that this loss of weight of 2/5 of the ligand is not as arbitrary as it seems but is a well-defined, precise quantity, independent of temperature. Indeed, at higher temperatures (Fig. 12) no stable product could be isolated, but still the same amount of mass is lost (2/5 LH_2) before the decomposition proceeds.

The thermal decomposition of $\text{Cu}(\text{LH}_2)\text{Br}_2$ gives no stable intermediate, clearly for the same reasons as given for the $\text{Cu}(\text{LH}_2)_2\text{Br}_2$ compound.

The ESR spectrum of $\text{Cu}(\text{LH}_2)\text{Cl}_2(\text{G})$ at room temperature shows only one broad featureless resonance at $g \approx 2$ [1]. Such signals are typical for copper(II) complexes exhibiting weak intermolecular coupling [9], while $\text{Cu}(\text{LH}_2)_2\text{Cl}_2(\text{E})$ gives well-resolved lines, characteristic for tetragonal distorted monomeric octahedral structures [10]. The magnetic moment of $\text{Cu}(\text{LH}_2)\text{Cl}_2(\text{G})$ is lower than the spin-only value for Cu(II) of 1.73 BM, again indicating a polymeric structure for this compound [11].

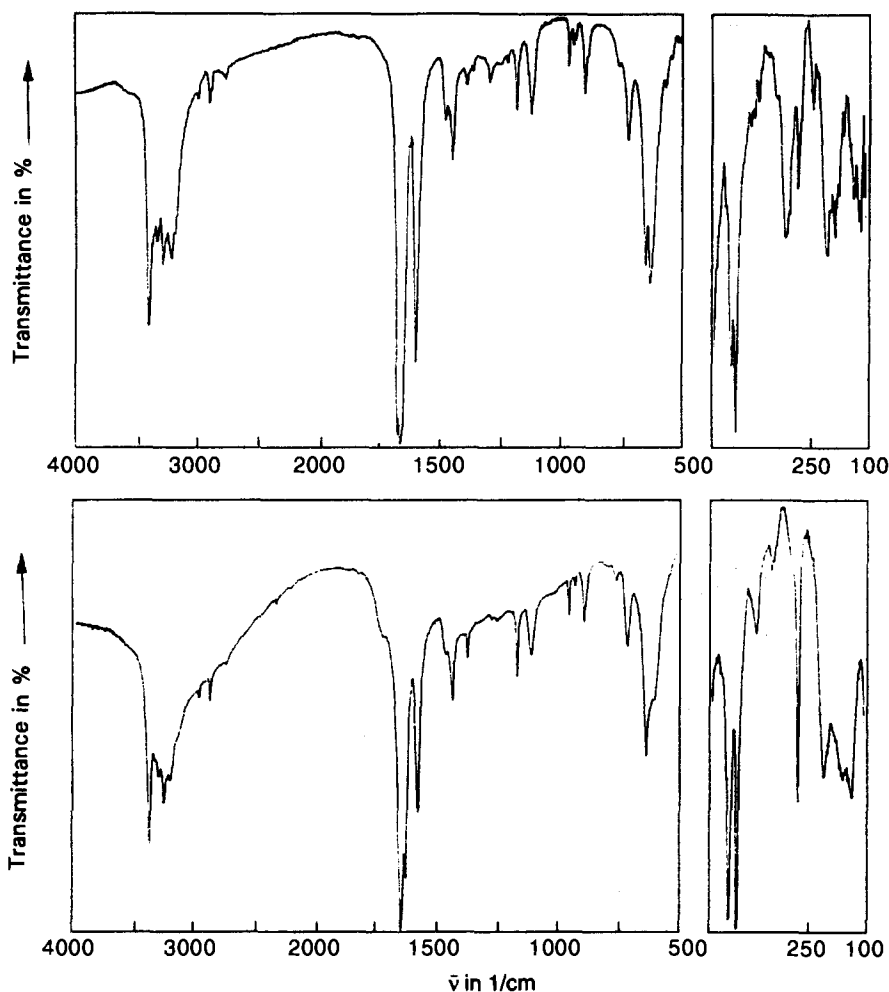


Fig. 10. IR spectra of $\text{Cu}(\text{LH}_2)_2\text{Cl}_2$ (E) (upper) and $\text{Cu}(\text{LH}_2)\text{Cl}_2$ (G) (lower).

The terminal halogen atoms in the monomeric $\text{Cu}(\text{LH}_2)_2\text{Cl}_2$ compound show relatively strong intermolecular $\text{N-H}\cdots\text{Cl}$ bridges [3]. As can be seen from the characteristic NH_2 fundamentals, displayed in Table 4, very strong hydrogen bonding to terminal chlorine atoms results in low values for the stretching mode and higher deformation modes in the monomeric complex, in comparison with the other compounds under investigation, where we observe practically no differences in position for the NH_2 fundamentals, indicating that there are no terminal halogen atoms available for the hydrogen bonding.

The mid-infrared spectra of $\text{Cu}(\text{LH}_2)_2\text{Cl}_2$ (G), prepared in the laboratory, of $\text{Cu}(\text{LH}_2)\text{Cl}_2$ (F) prepared by thermal degradation of the monomeric 1/2 complex, and of the intermediate H formed by decomposition of G, are all identical. In the

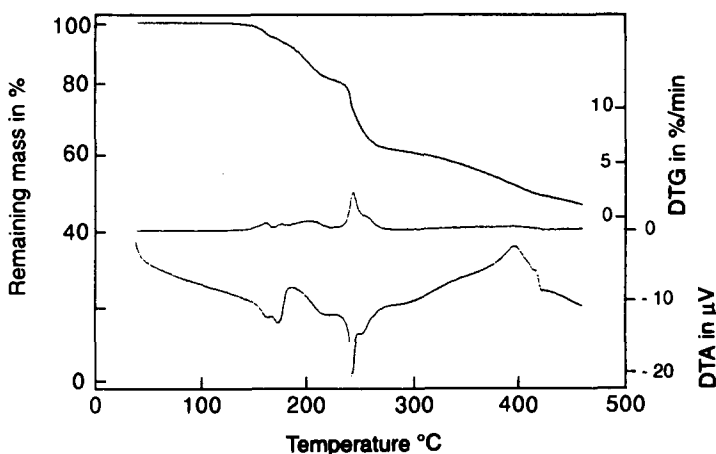


Fig. 11. TG, DTG and DTA curves for $\text{Cu}(\text{LH}_2)\text{Cl}_2(\text{G})$.

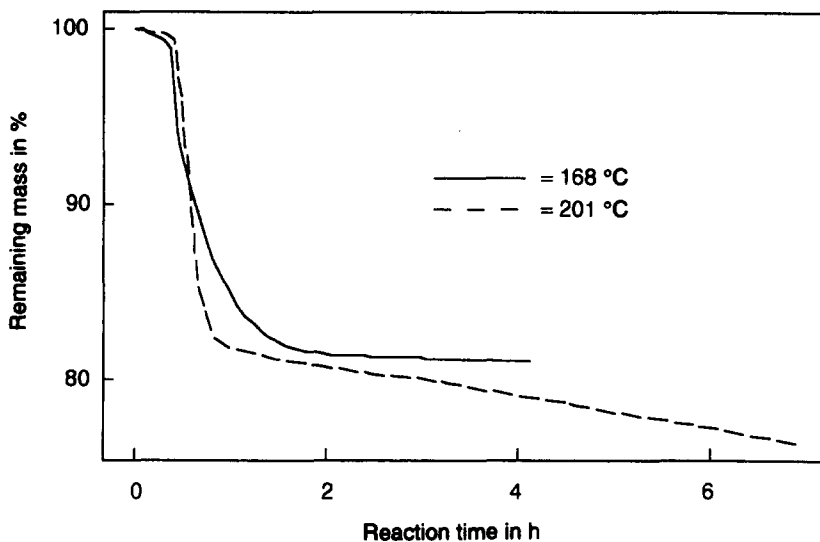


Fig. 12. Isothermal measurements on $\text{Cu}(\text{LH}_2)\text{Cl}_2(\text{G})$ at 168°C and 201°C .

far-infrared region of the two intermediates, we can observe similar bands; however the stoichiometric less malonamide in the intermediate formed from $\text{Cu}(\text{LH}_2)\text{Cl}_2$ is reflected in a more intense bridged $\nu(\text{Cu}-\text{Cl})$ mode. From these results we can conclude that these two intermediates and the $\text{Cu}(\text{LH}_2)\text{Cl}_2$ compound consist of polymeric structures with similar bonding of the ligand (identical mid-IR spectra), but the polymeric structures must be somewhat different, which becomes clear from the different far-infrared spectra.

Table 4
(NH₂) vibrations for some Cu(II) complexes

IR (cm ⁻¹)	$\nu_{as}(\text{NH}_2)$	$\delta(\text{NH}_2)$	$\tau(\text{NH}_2)$	$\nu(\text{Cu-X})$
Cu(LH ₂) ₂ Cl ₂ (E)	3290	1606	673	178
Cu(LH ₂)Cl ₂ (G)	3376	1592	624	136
Cu(LH ₂)Cl ₂ ^a (F)	3386	1589	620	142
Cu(LH ₂)Cl ₂ ^b (H)	3386	1588	620	142

^a Intermediate from Cu(LH₂)₂Cl₂.

^b Intermediate from Cu(LH₂)Cl₂.

Acknowledgements

S. De Beukeleer wishes to thank NFWO for financial support. The NFWO (Belgium) is also thanked for financial support towards the purchase of spectroscopic equipment used in this study. We are very grateful to Ing. J. Janssens for the thermogravimetric measurements.

References

- [1] S. De Beukeleer, H.O. Desseyn, S.P. Perlepes and E. Manessi-Zoupa, *Trans. Metal Chem.*, 19 (1994) 468.
- [2] I.I. Kalinichenko, N.M. Titov and L.A. Pecherskikh, *Russ. J. Inorg. Chem.*, 34 (1989) 1280, and Refs. cited therein.
- [3] S. De Beukeleer and H.O. Desseyn, *Spectrochim. Acta*, 50A (1994) 2291.
- [4] J.H. Flynn and L.A. Wall, *Plenum Lett.* 4 (1966) 323.
- [5] W. Wendlandt, *Thermal Analysis*, 3rd edn., Wiley, New York, 1986.
- [6] B.F. Little and G.J. Long, *Inorg. Chem.*, 17 (1978) 3401 and Refs. cited therein.
- [7] P.N. Hawker and M.V. Twigg, in G. Wilkinson, R.D. Gillard and J.A. McCleverty (Eds.), *Comprehensive Coordination Chemistry*, Pergamon Press, Oxford, 1978, Chap 44, pp. 1210–1211.
- [8] F. Basolo and R.C. Johnson, *Coord. Chem., Sci. Rev., Science Reviews*, 1986.
- [9] P. Illiopoulos and K.S. Murray, *J. Chem. Soc. Dalton Trans.*, (1988) 433.
- [10] B.J. Hathaway, *Coord. Chem. Rev.*, 35 (1981) 211.
- [11] F.A. Cotton and G. Wilkinson, *Advanced Inorganic Chemistry*, 5th edn., Wiley, New York, 1988.